



HAL
open science

A comparative study of degradation mechanisms of PBSA and PHBV under laboratoryscale composting conditions

Mélanie Salomez, Matthieu George, Pascale Fabre, François Touchaleaume, Guy Cesar, Anaïs Lajarrige, Emmanuelle Gastaldi

► To cite this version:

Mélanie Salomez, Matthieu George, Pascale Fabre, François Touchaleaume, Guy Cesar, et al.. A comparative study of degradation mechanisms of PBSA and PHBV under laboratoryscale composting conditions. *Polymer Degradation and Stability*, 2019, 167, pp.102-113. 10.1016/j.polymdegradstab.2019.06.025 . hal-03070279

HAL Id: hal-03070279

<https://hal.science/hal-03070279>

Submitted on 15 Dec 2020

HAL is a multi-disciplinary open access archive for the deposit and dissemination of scientific research documents, whether they are published or not. The documents may come from teaching and research institutions in France or abroad, or from public or private research centers.

L'archive ouverte pluridisciplinaire **HAL**, est destinée au dépôt et à la diffusion de documents scientifiques de niveau recherche, publiés ou non, émanant des établissements d'enseignement et de recherche français ou étrangers, des laboratoires publics ou privés.



Distributed under a Creative Commons Attribution - NonCommercial - NoDerivatives 4.0 International License

1 **A comparative study of degradation mechanisms of PBSA and PHBV under laboratory-**
2 **scale composting conditions**

3 **SALOMEZ Mélanie¹, GEORGE Matthieu³, FABRE Pascale³, TOUCHALEAUME**
4 **François¹, CESAR Guy², LAJARRIGE Anaïs¹, GASTALDI Emmanuelle^{1*}**

5
6 ¹*UMR IATE Ingénierie des Agropolymères et Technologies Emergentes, Campus INRA-SupAgro, 2 place Pierre*
7 *Viala, 34060 Montpellier, France*

8 ²*SERP BIO, Université Bretagne Sud, 56321 Lorient, France*

9 ³*Laboratoire Charles Coulomb, CNRS UMR-5221, Université de Montpellier, Place E. Bataillon, 34095*
10 *Montpellier, France*

11
12 **ABSTRACT**

13 Biodegradable plastics appear as one promising means to help solving the increasing issue of
14 environmental pollution by plastics. The present study aims at comparing the
15 biodegradation mechanisms of two promising biodegradable plastics, PHBV Poly(3-
16 hydroxybutyrate-co-3-hydroxyvalerate) and PBSA Poly(butylene succinate-co-adipate) with
17 the objective to provide a better understanding of the mechanisms involved and identify the
18 most relevant indicators to follow biodegradation. For this purpose, the progress of the
19 biodegradation process was monitored under controlled composting conditions at the
20 laboratory scale at 58°C using several methodological approaches for evaluating polymer
21 degradation. Indicators of the extent of material disappearance based on respirometry and
22 mass loss were combined to other indicators evidencing the morphological, structural and
23 chemical modifications induced at the surface or in the bulk of the material as surface
24 erosion by MEB and AFM, decrease of molecular weight by GPC, crystallinity changes by DSC
25 and chemical changes by ATR-FTIR. As expected, both polymers were rapidly biodegraded in
26 less than 80 days. However, in spite of its higher molecular weight and degree of crystallinity
27 PHBV degraded faster than PBSA, which led to suggest that different biodegradation
28 mechanisms would be involved. At this regard, a two-phase scenario was proposed for each
29 polymer on the strength of all the degradation-induced changes observed at the polymer
30 surface and in its bulk. Based on these two scenarios, the discrepancy in biodegradation rate
31 between PHBV and PBSA would be essentially attributed to significant differences in crystals
32 morphology and spatial organization of both polymers.

33 Regarding the relevance of the different indicators studied, mass loss stood out as the most
34 relevant and accurate indicator to assess the disappearance of material especially when
35 combined with respirometry and mineralization kinetics assessment. Besides, indicators
36 focusing on the surface changes as SEM, AFM and POM were emphasized since seen as
37 powerful tools to evidence morphological changes at different scales. At last, changes in
38 thermal properties as crystallinity rate and melting temperature, even if complex to
39 interpret due to the wide range of interdependent mechanisms they bring into play

40 appeared as inescapable tools for improving the understanding of the underlying
41 mechanisms involved in polymer biodegradation.

42

43 **KEYWORDS:** biodegradation, crystallinity, erosion, compost, Poly(3-hydroxybutyrate-co-3-
44 hydroxyvalerate), Poly(butylene succinate-co-adipate)

45 **1. INTRODUCTION**

46 With the increase of the global population, the demand for plastic materials in every aspect
47 of life and industry has become tremendous. As a result, the most of plastics produced
48 worldwide since 1950 (around 79%) has been accumulated in landfills or in the environment.
49 To face this environmental concern, which invariably causes injuries to ecosystems
50 equilibriums, biodegradable plastics, whether they derive from renewable feedstocks or
51 petroleum, are seen as promising means to help solving plastic waste management issues.
52 However, the global production capacities of biodegradable thermoplastics remains still very
53 low, estimated at 0.91 MT in 2018 (Source: European Bioplastics 2018) compared to the
54 348MT of total plastics produced worldwide in 2017 (Source: Plastics Europe Market
55 Research Group (PEMRG)). The biggest industrial sector using plastics is the packaging sector
56 (44.8% of total polymer resin production), they are also the primary waste producer
57 generating half of plastic wastes [1]. The most used polymers for packaging are polyethylene
58 (PE) and polypropylene (PP). But, their chemical stability is excessive in comparison with the
59 material lifespan required in the most of common everyday life usages where plastic is
60 needed (food packaging, single use products, cosmetics, etc.).

61 Among the biodegradable plastics suitable for replacing conventional plastics i.e. prone to
62 satisfy the requirements of a plastic for daily use in terms of functional and environmental
63 properties, aliphatic polyesters like polyhydroxyalkanoates (PHAs) and poly(butylene
64 succinate-co-adipate) (PBSA) are both interesting candidates. Nowadays global production
65 of PHAs and PBS/PBSA is respectively of 3.2% and 7.4% of all biodegradable polymers behind
66 starch blends, PLA and PBAT (Source: European bioplastic 2018). These two families have the
67 advantage to be totally or partially biosourced, which ensure a lower carbon footprint
68 compared to petrochemically derived plastics. PHAs belong to the family of biopolymers
69 synthesized by several bacteria as intracellular carbon and energy storage granules. A wide
70 variety of prokaryotic organisms can accumulate PHAs from 30 to 80% of their cellular dry
71 weight by fermentation using various renewable feedstocks. PHAs have 150 different types
72 of monomers allowing the tuning of their physical properties from crystalline–brittle to soft–
73 sticky materials depending on the length of the side aliphatic chain at the chiral carbon [2].
74 PHAs and more specifically Poly(3-hydroxybutyrate-co-3-hydroxyvalerate) known as PHBV
75 have interesting oxygen and water vapour barrier properties compared to other
76 biodegradable polymers, thus making it a good candidate for food packaging applications [3]
77 [4]. PBS and its copolymers are a family of biodegradable polymers with excellent

78 biodegradability, thermoplastic processability and balanced mechanical properties [5]. Its
79 relatively good processability via a broad range of conventional techniques (i.e. sheet
80 extrusion, injection molding, thermoforming, blow molding, foaming, fiber spinning, and
81 filament) renders it suitable for the production of various materials designed for daily use
82 (packaging, automotive, textile, and sports and leisure industries). Poly(butylene succinate-
83 co-adipate) known as PBSA is synthesized from 1,4-butanediol, succinic acid and adipic acid
84 monomers by copolymerization. In the past, all the monomers constituting PBSA were
85 exclusively derived from fossil raw materials. However, with the development of biorefinery
86 throughout the world, these key biobased chemical building blocks are more and more
87 obtained by fermentative production routes based on renewable feedstocks of second
88 generation (dextrose, glucose, sucrose, biobased glycerol, and vegetable oil).

89
90 PHBV and PBSA polyesters have very good biodegradability performances in various
91 environments compared to other biodegradable polymers [6-8]. Poly(3-hydroxybutyrate) is
92 actually considered as a suitable alternative for cellulose as a reference material in the
93 standards of biodegradation for soil and water environments, respectively NF EN 17033 and
94 ISO DIS 14852. Copolymerization is one of the strategies used to improve biodegradability
95 and tune functional performances. Increasing hydroxyvalerate content in PHBV decreases its
96 melting temperature, elastic modulus and tensile strength with higher elongation at break
97 up to 970% [9] and improved biodegradability [10]. In the same way, the copolymerisation of
98 PBS with butylene adipate monomers up to 60% increases chain mobility and
99 biodegradability of the copolymer by lowering both crystallinity and melting temperature
100 [11]. Within available commercial PHBV, P(3HB-co-3HV) material at molar percentage of HV
101 is very brittle with high elastic modulus, low tensile strength and an elongation at break
102 around 3%, thus making it a strong and hard material [12]. Among commercially available
103 PBSA polyesters, P(BS-co-BA) at 20%mol BA displays a good compromise between
104 biodegradation and mechanical performances (tensile strength and elongation at break of
105 430%) [5].

106
107 The ability of polymers to biodegrade is driven by several parameters related to intrinsic
108 chemical and physical properties as emphasized by enzymatic degradation studies [13].
109 Among them, not only their chemical composition and first order structure (molecular
110 weight and distribution, degree of branching) are expected to be involved but also their
111 physical state including higher order structures (glass transition temperature, melting
112 temperature, modulus of elasticity, degree of crystallinity, crystals size and structure)
113 together with their surface properties (hydrophobicity, roughness, specific surface). Beside
114 the role played by the intrinsic material properties on biodegradation performances, the
115 environmental conditions including both abiotic phenomena (UV, oxidation, mechanical
116 stress) and biotic ones are also important parameters to be focused on. While abiotic
117 phenomena lead to the damage and fragmentation of a polymer by oxidation and hydrolysis
118 mechanisms only biotic phenomena will result into the complete mineralization of a

119 polymer. The primary prerequisite that drives the biodegradation of plastics lies on the
120 adherence of microorganisms on the surface of plastics followed by the colonization of the
121 exposed surface and the formation of a biofilm. Afterwards, plastics are enzymatically
122 degraded in a two-step process: first the enzyme binds to the surface of the plastic substrate
123 and secondly, the enzymatic catalysis of the hydrolytic cleavage resulting in the reduction of
124 the polymer chain length into low molecular weight oligomers, dimers and monomers [14].
125 Once polymer chains are short enough, they can be assimilated by microorganisms and
126 ultimately converted aerobically into biomass, water and CO₂. The second requirement that
127 should be fulfilled for considering a polymer as biodegradable in a given environment is thus
128 the presence in the medium of microorganisms able to synthesize and release (exo)-
129 enzymes able to degrade this polymer. In that respect, as established for a long time by
130 Tokiwa and Suzuki (1977), the ability of polyesters to biodegrade comes from their
131 susceptibility to be hydrolyzed by lipases or esterases, which are ubiquitous enzymes in the
132 environment.

133 To our knowledge, no studies have compared the biodegradation performance of different
134 families of biodegradable polymers in controlled environmental conditions while also
135 studying the underlying mechanisms. The results of Yang et al. [8] have shown that PBSA and
136 PCL biodegraded better than other polymers (PP, PLLA, PBS) in the same compost but the
137 performance and mechanisms of biodegradation were not further investigated. The study of
138 Mercier [7] compared the degradation of different polymers (EVOH, PP, PBAT, PET, PBS, scl-
139 PHA, PLLA, PA66) in an uncontrolled compost simulating home composting conditions
140 (average temperature of 13°C) and found that PBS and scl-PHA were the polymers which
141 degraded the most with a mass loss of 5.5 and 8%, respectively after 450 days of incubation.
142 Discrepancy in degradation performances of the polymers tested was mainly attributed to
143 the formation of higher cell density biofilms and their specific surface properties. Other
144 studies have focused on the degradation of a single polymer in laboratory composting
145 conditions. However, results are difficult to compare due to the use of different
146 experimental conditions, *i.e.* different kind of compost and inoculum, and also because of
147 different processes to obtain polymer films (hot pressing, casting or extrusion).
148 Biodegradation of PHBV has been extensively studied in composting conditions [15-20] in
149 contrast to studies dealing with the biodegradation of PBSA, which are still scarce [8, 21].
150 Furthermore, it is rare to see different methodological approaches to evaluate polymer
151 biodegradation. Most of these studies generally focused on changes in mass loss without
152 monitoring in parallel the carbon dioxide released by the material during its degradation. It
153 is however worth noting that evidencing polymer mass loss does not guaranty its final
154 assimilation by microorganisms.

155 In this context, the present study aims to compare the biodegradation performance and
156 mechanisms of films made of PHBV and PBSA under controlled composting conditions at the
157 laboratory scale. This comparison between these two promising biodegradable polymers
158 could help to identify key limiting factors driving biodegradation. For this purpose, initial

159 surface properties of both films were characterized and the progress of the biodegradation
160 process was monitored using several methodological approaches for evaluating polymer
161 degradation. Indicators of the extent of material disappearance (assessed by respirometry
162 and mass loss measurement) were combined to other indicators evidencing the
163 morphological, structural and chemical modifications induced at the surface or in the bulk of
164 the material (surface erosion, chain molecular weight decrease, crystallinity and chemical
165 changes). Correlating such approaches could not only help identifying the key parameters
166 explaining the differences in biodegradability between the two polymers but would also
167 contribute to evidence indicators that could be considered as relevant quantitative
168 descriptors for evaluating the progress of the biodegradation process.

169 **2. MATERIALS AND METHODS**

170 **2.1 Materials**

171 The PHBV and PBSA pellets were purchased from Natureplast (France) under the trade
172 names PHI002 and PBE001, respectively. PHBV contains 1-3 mol% of hydroxyvalerate (HV)
173 and contains boron nitride as nucleating agent. PBSA contains 21 +/- 1 mol% of butylene
174 adipate (BA) and is 31% biosourced. Cellulose microcrystalline powder, soda and
175 hydrochloric acid were purchased from Merck. Formamide and diiodomethane were
176 provided by Acros organics (Geel, Belgium), ethylene glycol and hexamethyldisilazane were
177 purchased from Aldrich chemical Co. Inc. (Milwaukee, USA).

178 PHBV and PBSA pellets were extruded using a twin-screw extruder (Thermo Scientific™
179 EuroLab 16) with an L/D ratio of 40 and a screw diameter of 16 mm equipped with a flat die
180 and calendaring. The processing conditions used were a screw speed of 200 rpm, a flow rate
181 of 1 kg/h and temperature profiles from 140 to 180°C for PHBV and 100 to 135°C for PBSA.
182 PHBV and PBSA films displayed a thickness of 175 +/- 25 µm and 210 +/- 25 µm, respectively.

183 **2.2 Biodegradation tests**

184 Respirometric tests were conducted using a method adapted from NF ISO 14855 standard to
185 evaluate the biodegradation kinetic of PHBV and PBSA films in composting conditions. For
186 this purpose, mature green compost was collected in the waste management centre of
187 Aspiran (France) and sieved through 5 mm meshes. Biodegradation tests were carried out in
188 cylindrical hermetic glass vessels (1000 mL capacity) containing three small open
189 polypropylene flasks (60 mL capacity). The first flask contained 6 g of wet compost with final
190 water content of 50%, (pH of 8.05 and C/N ratio of 26.6), mixed with an equivalent of 50 mg
191 carbon of each tested film previously cut in 8 x 8 mm pieces. The second flask contained 30
192 mL NaOH solution (0.1 M) to trap the CO₂ produced by microorganisms, and the third flask
193 contained distilled water in order to maintain the relative humidity at 100% inside the
194 vessel. The blank control was composed only of compost. Cellulose microcrystalline powder
195 was used as positive control. The blank and positive controls were done in triplicate whereas
196 each test sample of PHBV and PBSA film was repeated twelve times. All the samples were
197 incubated in the dark at 58±1°C during 120 days. At selected time interval, NaOH flasks were

198 removed from the vessel to be titrated and were then replaced by new flasks containing
199 NaOH. At the same time and during the first 41 days of incubation, one flask containing a
200 test sample of both films was recovered to ensure mass loss measurements and further
201 analysis. The compost humidity was maintained constant by adding distilled water all along
202 the experiment. The percentage of mineralization of a test sample was determined as the
203 ratio of the amount of carbon dioxide released from the material mineralization related to
204 the maximum theoretical amount of carbon dioxide that could be released by the test
205 material using Equation (1):

$$206 \quad \textit{Mineralization} (\%) = \frac{n_{\text{CO}_2 \text{ test}} - n_{\text{CO}_2 \text{ blank}}}{n_{\text{CO}_2 \text{ theoretical}}} \quad (1)$$

207 Where, $n_{\text{CO}_2 \text{ test}}$ is the amount of CO_2 released by the respiration of the compost medium and
208 the mineralization of the material, $n_{\text{CO}_2 \text{ blank}}$ is the amount of CO_2 released by the compost
209 medium only, and $n_{\text{CO}_2 \text{ theoretical}}$, the maximal theoretical amount of CO_2 released by the
210 mineralization of the material calculated by using its carbon content. Biodegradation curves
211 with no priming effect were selected and modelled using Hill and Boltzmann equations [22].

212 **2.3 Mass loss**

213 The PHBV and PBSA films removed from the compost throughout the biodegradation
214 process (at day 6, 10, 15, 20, 29, 41) were carefully soaked 5 min in ethanol 70% and then
215 rinsed with distilled water to remove all the particles. Finally, samples were dried overnight
216 at 60°C under vacuum and weighted using an electro balance to determine the percentage
217 of mass loss using Equation (2):

$$218 \quad \textit{Mass loss} (\%) = \frac{m_0 - m_f}{m_0} \times 100 \quad (2)$$

219 Where, m_0 is the mass of the material before biodegradation and m_f the mass after
220 biodegradation.

221 Prior to the subsequent analyses (see below), an ultra-sound treatment was applied to the
222 dried specimens to remove any residual organic matter and microorganisms from the
223 surface. For this purpose a sonicator (Qsonica Q700) with a microtip probe was used during
224 1 min repeated 3 times (amplitude of 30%) and a rest time of 2 min between each run.

225 **2.4 Surface properties: contact angle measurements and atomic force microscopy**

226 Surface properties of pristine PHBV and PBSA films were determined by contact angle
227 measurements performed at 25°C using a goniometer (Digidrop, GBX, France) equipped with
228 a CCD camera (25 frames/sec) and the GBX software (Windrop, GBX, France). The dispersive
229 (γ_s^d) and polar (γ_s^{AB}) components of the solid surface tension were evaluated by applying the
230 Owens-Wendt approach [26]. For this purpose, four reference liquids were used:
231 formamide, diiodomethane and ethylene glycol. Their respective surface tension
232 components were taken from the literature and are listed in Table 1 [23-24].

233 Atomic force microscopy (AFM) was performed on each sample to get accurate insight of the
234 initial surface state of both polymers. Characteristic image of respective area, $10 \times 10 \mu\text{m}^2$
235 and $50 \times 50 \mu\text{m}^2$, were acquired for each sample using a Nanoscope V (Bruker instruments,
236 Madison, WI, United States) in contact mode (Binnig et al., 1986) and standard silicon
237 probes (Bruker, DNP). Root mean square (RMS) roughness of the polymer surface was
238 measured for each scale with Gwyddion software after subtraction of the average plane.

239 **2.5 Scanning Electron Microscopy (SEM)**

240 SEM observations were performed using a field emission scanning electron microscope
241 (FESEM S-4500, Hitachi, Japan) with an acceleration voltage of 2 kV secondary electrons.
242 PHBV and PBSA film samples were either directly mounted on stub using carbon conductive
243 tape and then coated with gold/palladium by ion sputtering, or previously cryo-fractured
244 under liquid nitrogen, depending on the observation that was done on the film surface or its
245 cross-section, respectively.

246 **2.6 Fourier Transform InfraRed spectroscopy (FTIR)**

247 PHBV and PBSA films were analysed using an infrared spectrometer (Thermo Scientific,
248 Nicolet 6700) and a DTGS-KBr detector in Attenuated Total Reflectance (ATR) mode. FTIR-
249 ATR spectra ranged from 4000 to 800 cm^{-1} with a resolution of 2 cm^{-1} and were averaged over
250 32 scans. Carbonyl index were calculated by normalizing the area of each peak over the area
251 of a reference peak, respectively 1473 cm^{-1} for PBSA (-CH- symmetric deformation [25]) and
252 1379 cm^{-1} for PHBV (-CH₃ symmetric wagging [26, 27]) after correction of the spectral
253 baseline.

254 **2.7 Molecular weight**

255 The PHBV and PBSA film samples prepared as described above were dissolved in chloroform
256 at a concentration of 5 mg/ml. PBSA dissolved immediately whereas PHBV samples needed
257 to be heated to 50°C and agitated for 1-2h until complete dissolution arrived. Resulting
258 solutions were then filtered through a $0.45 \mu\text{m}$ polytetrafluoroethylene (PTFE) syringe filter.
259 Molecular weights were measured by GPC (Waters system) at 35°C using a PLgel Mixed C-
260 $5\mu\text{m}$ -2x300m column and a refractive index (RI) detector. Chloroform was used as an eluent
261 at a flow rate of 1 ml/min. The number-average (M_n) and weight-average (M_w) molecular
262 weights were calculated using a calibration curve from polystyrene standards. The scission
263 index [28] was calculated from the following Equation (3):

$$264 \quad SI = \frac{Mn_{(t=0)}}{Mn_{(t)}} - 1 \quad (3)$$

265 Where $Mn_{(t=0)}$ and $Mn_{(t)}$ are the initial number-average molecular weight and the number-
266 average molecular weight at a given time of biodegradation, respectively. In our study, the
267 scission index was calculated between day 6 and day 41.

268 **2.8 Differential Scanning Calorimetry (DSC)**

269 Thermal analyses were carried out on 5-8 mg of PBSA and PHBV films collected from the
270 compost at different time intervals using a TA instrument DSC Q200 under nitrogen
271 atmosphere. A thermal ramp of 5°C/min was used during the first run of heating and the
272 second run of cooling with a temperature ranging from -40°C to 150°C and -40°C to 200°C,
273 respectively. The crystallinity degree of samples was calculated from thermograms using
274 Equation (4):

$$275 \quad X_c(\%) = \frac{\Delta H_m}{\Delta H_m^0} \times 100 \quad (4)$$

276 Where, ΔH_m is the melting enthalpy and ΔH_m^0 the melting enthalpy of the polymer
277 supposed to be 100% crystalline, *i.e.* 110.3 J/g for PBSA [29] and 146 J/g for PHBV [30]. The
278 highest peak of the melting scan of pristine PHBV and PBSA was used to calculate their
279 respective melting temperature.

280

281 **3. RESULTS**

282 **3.1. (Bio)degradation kinetics under laboratory-scale composting conditions**

283 The biodegradation rate of PHBV and PBSA films was monitored by concomitantly measuring
284 the released carbon dioxide (Fig. 1) and the weight loss (Fig. 2). To ensure an accurate
285 comparison between the two measurements, several respirometric tests have been
286 launched simultaneously, one of them being periodically interrupted for weight loss
287 measurement and complementary analysis. Beyond 40 days of incubation, measurements
288 on plastic specimens could not be further performed. The degradation was too far advanced
289 to ensure the proper collection of the sample, the films breaking into small pieces, which
290 became impossible to recover from the composting medium. In contrast to weight loss
291 measurement, respirometric tests allowed monitoring biodegradation until the complete
292 mineralisation of the material.

293 The biodegradation curves and weight loss measurements (Fig. 1-2) confirmed that both
294 polymers were fully biodegradable, *i.e.* that the entire material was fully mineralised into
295 carbon dioxide attesting its final assimilation by microorganisms. This was confirmed by the
296 plateau phase reached by the evolution of carbon dioxide similar to the positive control
297 (cellulose), which reflected that no further biodegradation was expected. The mineralization
298 rates of PHBV and PBSA specimens reached 100% after 70-90 days of incubation (Fig. 1).

299 The evolution of mass loss in Figure 1 could be divided in two phases, each being
300 characterized by a different kinetic of degradation. During the first phase (0-20 days), the
301 degradation of PHBV was faster than for PBSA and increased exponentially over time. At the
302 end of this phase, mass loss was five times higher for PHBV than for PBSA, with 50% against
303 10%, respectively. After 20 days of incubation, both degradation rates changed with a slow
304 down for PHBV whereas an acceleration was observed for PBSA. This change in degradation

305 kinetics could also be evidenced on the mineralisation curves, resulting in two different
306 types of modelling; a (single) sigmoidal shape according to Hill equation for PHBV *versus* a
307 double sigmoidal shape curve fitting with Boltzmann equation for PBSA. Despite the
308 increased rate of degradation of PBSA, its overall degradation kinetic remained slightly
309 slower than these of PHBV. As a consequence, the plateau phase of respirometric curves was
310 reached earlier for PHBV than for PBSA. As an illustration of such differences no pieces of
311 PHBV film could be recovered in the compost in contrast to 5-10% residual material
312 weighted for PBSA at the last sampling. The good correlation found between respirometric
313 and mass loss curves until 40 days indicated that the mass loss of both material was
314 essentially due to the conversion of organic carbon in carbon dioxide without implying any
315 leaching phenomenon.

316 Figure 1

317 Figure 2

318

319 **3.2. Surface morphological and macrostructural modifications**

320 Surface polarity, RMS roughness and 3D topography of both pristine polymer films have
321 been investigated using contact angle measurements and AFM (Table 1). Such properties are
322 known to be key parameters driving the adhesion of microorganisms and controlling biofilm
323 formation on a material surface [31, 32]. The surface properties of pristine PHBV and PBSA
324 films indicated that PBSA was slightly more hydrophilic than PHBV as reflected by a higher
325 relative polar component ($\gamma_S^{AB}/\gamma_S = 13\%$ for PBSA against 10% for PHBV) and also a higher
326 water wettability as indicated by a contact angle value (θ) of 68.2° for PBSA against 76° for
327 PHBV. However, despite these small but significant differences, it could be assumed that
328 both polymers exhibited rather close surface properties in terms of surface energy.

329 By contrast, the surface morphology of the pristine PHBV and PBSA films evidenced by AFM
330 exhibited contrasted scales of structuring with a different surface roughness depending on
331 the scale considered (Table 1). As shown on AFM 3D pictures, PHBV surface was covered by
332 compacted spherical structures displaying a diameter around 10-15 μm and that could be
333 ascribed to spherulites [33]. Such a structural organization led the RMS value to decrease
334 from 230 to 58 nm when reducing the scale from 50 to 10 μm . In contrast, PBSA presented a
335 surface made of numerous asperities of a few micrometres height whatever the considered
336 scale. Thus, even if PHBV and PBSA exhibited quite similar roughness values at 50 μm scale,
337 AFM images and roughness values obtained at 10 μm scale clearly showed that PBSA had
338 initially a surface 20-times rougher than PHBV.

339

340 Table 1

341

342 To follow macroscopic modifications occurring at the surface of both polymers during the
343 progress of the biodegradation process, MEB images were performed on films sampled from
344 the compost medium at different time intervals. MEB images in figure 3 showed the time-
345 evolution of the surface erosion for PHBV and PBSA. Comparison between both polymers
346 revealed a stronger degradation of the PHBV film surface than for PBSA. Such surface
347 erosion that could be compared to an enzymatic etching evidenced significant differences in
348 the crystal organisation of each polymer. In PHBV, spherulites with highly ordered lamellae
349 became clearly visible only 10 days after starting the incubation in compost (Figure 3c). This
350 primary stage of surface erosion could be ascribed to a faster degradation of amorphous
351 phase in comparison with crystalline phase as generally reported in literature regarding
352 enzymatic degradation of plastics [13]. By contrast, the surface erosion of PBSA revealed a
353 different kind a structure. In early degradation stages, flat layers of crystals were observed
354 (Figure 3f).

355 Figure 3

356 Images obtained at a lower magnification (Figure 4) indicated that this erosion phenomenon
357 occurred heterogeneously at the surface leading to the formation of erosion patterns.
358 Comparison between both polymers revealed footprints of microbial filaments on the
359 surface of PHBV films as seen in figure 4a, whereas these filaments were absent or scarcely
360 observed on PBSA films. These footprints appeared as the starting points of surface
361 degradation as evidenced on figure 4b. Colonization of PHBV by fungi could thus have been
362 more important than for PBSA. Such differences could be linked with the differences in
363 roughness evidenced at small scale by AFM (Table 1). It has been previously reported that
364 microbial communities of plastics, the plastisphere, would be specific for each plastics [7].

365 Figure 4

366 To complete this microstructural investigation, a macroscopic analysis of the degradation-
367 induced physical changes was undertaken at a higher scale of observation. As illustrated in
368 Figure 5, two different degradation behaviours were observed with the formation of holes
369 for PHBV whereas PBSA fragmented after around 20 days of incubation. These differences in
370 morphology were confirmed by SEM images of both films incubated 41 days in compost
371 medium revealing that PHBV displayed a clear tendency to become porous with an eroded
372 shape, whereas PBSA tended to fracture with the formation of sharp edges (Figure 6). This
373 propensity to fragment as a distinctive feature to PBSA has already been reported by
374 Puchalski et al. [21] when studying the degradation of PBSA in compost conditions.

375 Figure 5

376 Figure 6

377

378 **3.3. Surface physico-chemical modifications during composting**

379 ATR-FTIR measurements were performed at the surface of PBSA and PHBV films (from 0.5 to
380 5 μm deep depending of the wavelength) collected from the compost medium over time
381 during 40 days with the aim to evidence the chemical modifications induced by the
382 biodegradation process. Based on the structure of polyesters, hydroxyl (OH) and carbonyl
383 (C=O) groups could be used as tools to study degradation and hydrolysis of ester linkages
384 [16, 19, 34]. In the present study, the peak usually ascribed to OH groups (3350 cm^{-1} free -OH
385 stretching) was not taken into account since rather affiliated to the presence of water. The
386 presence of this peak was also associated with a peak at 1650 cm^{-1} corresponding to the C=O
387 stretch of amide functions probably due to the presence of proteins from microorganisms
388 (results not shown). To remedy these artefacts, all the films samples were subjected to an
389 ultrasound treatment and a drying prior to FTIR analysis to remove microorganisms and
390 water.

391 Evolution of carbonyl index of PHBV and PBSA films during incubation in compost medium is
392 given in Figure 7. The carbonyl index of PHBV ($1770\text{-}1700\text{ cm}^{-1}$) was stable during the first 20
393 days of degradation in compost suggesting no accumulation at the film surface of carbonyl
394 groups resulting from the ester linkage hydrolysis (Fig. 7). Thus, it can be supposed that the
395 oligomers produced by the enzymatic hydrolysis of the polymer were probably immediately
396 assimilated by microorganisms or leached in the compost medium, hydrolysis and erosion
397 being probably concomitant in this first phase for PHBV. Luo et al. [16] and Weng et al. [19]
398 who studied biodegradation in compost medium of PHBV and PHAs, respectively, also
399 concluded that the chemical structure of residual material surface remained unchanged
400 during the degradation process. By contrast during the second degradation phase (>20 days)
401 the carbonyl index of PHBV started to decrease. This could suggest that after 20 days
402 oligomers produced by the enzymatic hydrolysis of ester linkages remained at the film
403 surface since not easy to release in the medium and/or not rapidly consumed by bacteria.
404 The evolution of carbonyl index of PHBV during this second phase could be related with the
405 slow down in mass loss and respirometry that also occurred after 20 days.

406 For PBSA, a different behaviour was observed at the film surface with a decrease of the
407 carbonyl index ($1770\text{-}1690\text{ cm}^{-1}$) during the first 20 days and no change afterwards (Fig. 7).
408 Enzymatic hydrolysis of the ester linkages during this first phase did not lead to a leaching of
409 the oligomers that would increase mass loss. This could explain the lower erosion rate of
410 PBSA during the first phase. During the second phase (>20 days), the decrease of the
411 carbonyl index slowed down suggesting that the hydrolysis was concomitant with the
412 leaching of oligomers chains. This could explain the higher rate of mass loss in this second
413 phase of degradation.

414 Figure 7

415

416 **3.4. Bulk structural modifications**

417 Changes in bulk properties of both polymer films during biodegradation were firstly assessed
418 through the evolution of their number-average molecular weight (M_n) molecular weight as a
419 function of degradation time in compost (Fig. 8). The results indicated PHBV was initially
420 roughly twice higher than for PBSA with M_n values of 94000 versus 44000 ± 3000 g/mol. A
421 linear decrease in M_n values was observed according to time, which was accompanied a
422 more or less pronounced reduction in the polydispersity depending on the considered
423 polymer. The polydispersity index of PBSA was initially equal to 7.5, and then it rapidly
424 decreased to 3.3 at 6 days and finally stabilized around 2.6 after 41 days incubation in
425 compost. Regarding PHBV, changes in dispersity were weaker with values varying from 2.38
426 to 2.2 during the degradation time in compost. The decrease in M_n is a typical consequence
427 of the biodegradation process that reflected bulk changes rather than surface erosion that
428 would be induced by degrading enzymes [35] [36] [21]. This assertion is based on the rather
429 low specific surface of the polymer films tested in the present study (thickness of 175-210
430 μm) together with the fact that enzymes produced in the compost medium were not
431 supposed to diffuse into the bulk of the material due to their steric hindrance. As a
432 consequence the decrease in M_n mainly provided an indication of the involvement of
433 hydrolytic chain scission mechanisms resulting in a noticeable size chains reduction.

434 However, the decrease in polydispersity index led to suggest that another degradation
435 mechanism would be implied. According to Puchalski [21] the reduction of polydispersity
436 index would be due to the enzymatic etching of oligomers from the film surface, these
437 latters would be small enough to diffuse and would be finally released in the compost
438 medium. The combination of a relatively slow hydrolysis of high M_n polymers and a faster
439 enzymatic cleavage of oligomers and low M_n polymers would lead M_n and polydispersity to
440 decrease concomitantly. This also accounted for the rapid decrease of the polydispersity
441 index of PBSA during the first days of incubation in compost. The distribution profile of
442 polymer chains exhibited a population of short chains (<4000 g/mol) that quickly
443 disappeared during incubation in compost. These short chains were probably expected to
444 diffuse through the material and were quickly leached, which is in accordance with previous
445 studies [37] [38].

446 Figure 8

447 During degradation in compost medium the scission index also increased linearly with a rate
448 2.5 times higher for PBSA than for PBHV (Fig. 9). Scission index value being closely associated
449 with the ability of ester linkages to be hydrolysed by the water contained in the compost
450 medium, this indicator is thus expected to increase with the water permeability and water
451 diffusion of polymers. According to data reported in literature PBSA exhibited a higher water
452 permeability and water diffusion coefficient than PHBV, with P values of 6787 barrer against
453 149 barrer [39] [40], and D_0 values of $2.0 \cdot 10^{-8}$ $\text{cm}\cdot\text{s}^{-1}$ against for $3.3 \cdot 10^{-11}$ $\text{cm}\cdot\text{s}^{-1}$ [41][40] for
454 PBSA and PHBV, respectively. It is worth noting that all the polymers used in these studies
455 were of the same commercial grade as those of the present study. Based on these data, one

456 can infer that water molecules would diffuse more rapidly in the PBSA film than in the PHBV
457 one. The evolution of the number-average molecular weight of polymer chains reflecting a
458 degradation phenomenon mainly induced by liquid water used for hydrolysis reaction, index
459 scission was found to be higher in the PBSA film than in the PHBV one.

460 Figure 9

461 The next step in the analysis of the degradation-induced changes in the bulk of the polymer
462 films was the investigation of their thermal properties. The results deduced from the DSC
463 measurements of PHBV and PBSA films as a function of degradation time in compost are
464 reported in Figure 10 and 11. The crystallinity ratio of initial films appeared slightly different
465 with X_c value for PBSA being lower ($46.7 \pm 1\%$) than for PHBV ($53.6 \pm 0.7\%$). Over the first 40
466 days of incubation in compost the evolution of crystallinity indicated significant differences
467 between both polymers. An increase of crystallinity of 23% was recorded for PBSA films
468 whereas only a slight increase of 2.4% was observed for PHBV. These results supported the
469 fact that amorphous phase would be preferentially degraded during composting for PBSA
470 films thus increasing the crystallinity ratio, whereas for PHBV both amorphous and
471 crystalline phase would be equally degraded. It could also be hypothesised that crystals of
472 PHBV would be more easily degraded than the crystals of PBSA due to significant differences
473 in their surface structure, morphology and chain mobility [42].

474
475 Iggui et al. [20] also reported a significant reduction of M_w during degradation of PHBV in
476 compost whereas no change in crystallinity was observed. However, no abiotic hydrolysis
477 control was performed to evaluate the respective contribution of hydrolytic and enzymatic
478 degradation. Rutkowska et al. [17] reported that PHBV films degraded via enzymatic process
479 with a slight influence of the hydrolytic process. The weak decrease of M_w (8% in two
480 weeks) obtained by these authors suggested that the bulk of the material could also be
481 affected during the biodegradation process. But, the hydrolytic process could have been
482 slower due to different experimental composting conditions as uncontrolled parameters and
483 a lower average temperature (21°C against 58°C in the present study). In contrast, Luo et al.
484 [16] and Weng et al. [18] observed neither change in the M_w , nor changes in crystallinity
485 during degradation in compost. Regarding the degradation-induced changes in compost
486 Puchalski et al. [21] also observed an increase of the crystallinity of PBSA with a concomitant
487 decrease of the molecular weight. These authors concluded that the increase in crystallinity
488 was a result of both the hydrolysis and enzymatic degradation with a degradation of
489 amorphous parts being first followed by crystalline ones.

490
491 Besides the assumption based on a differential accessibility of the crystalline phase of both
492 polymers by degrading enzymes that will be developed below, recrystallization phenomenon
493 could also be evoked to account for the increased crystallinity rates during the
494 biodegradation process. As evoked above, water-induced hydrolysis of polymer chains
495 occurred in the bulk of both polymers in the first stage of incubation. Such chain cleavages

496 were expected to provide an extra mobility to the oligomers and shortened polymer chains,
497 especially those that are entrapped in the bulk of the film, leading them to crystallise and/or
498 the remaining crystalline phase to reorganise, giving rise to an increase in crystallinity [43].

499 This assumption was supported by the DSC thermograms of PHBV and PBSA films (Fig. 11),
500 which showed two melting peaks evolving conversely over time, the enthalpy of the first
501 melting peak decreasing while the second one increases. Based on these results one can
502 infer that a reorganization of the crystalline phase of the two polymers occurred during
503 incubation in compost medium. It is worth noting that the rather high temperature (58°C)
504 set in the compost medium combined with a relative humidity close to 100% were
505 conditions prone to promote the reorganisation of the crystalline phase. Iggui et al. [44] also
506 reported the formation of a double melting peak and a decrease of the melting temperature
507 of PHBV films subjected to photo-oxidation. These changes were attributed to the formation
508 of new crystal populations with different morphologies and dimensions together with a
509 reduction in molecular weight of PHBV polymer chains. During the degradation process, it
510 could be supposed that the structure of PHBV evolved toward a lower ordered structure of
511 crystal and shorter polymer chains as supported by the decrease of the melting
512 temperatures (Fig. 11). On the contrary, the increase in melting temperature observed for
513 PBSA over the degradation process reflected a lower flexibility of polymer chains and a
514 higher level of structuration of the crystals as reflected by the increased degree of
515 crystallinity. These structural changes could also explain the ability of PBSA to fragment
516 during degradation in compost.

517 **4. GENERAL DISCUSSION**

518 As expected PBSA and PHBV films were rapidly biodegraded (60 to 80 days) in lab-scale
519 composting conditions. But, PHBV degraded faster than PBSA in spite of its higher molecular
520 weight (Fig. 8) and degree of crystallinity (Fig. 9) together with quite similar surface
521 hydrophilicity (table 1). This led to suggest that different biodegradation mechanisms would
522 be involved depending on the polymer tested. For this purpose, a two-phase scenario was
523 proposed for each polymer. In both cases, the loss of material appeared mostly driven by
524 enzymatic erosion occurring at the surface of each material with a weaker contribution of
525 hydrolytic chain scission mechanisms induced by water diffusion that mainly affected the
526 bulk of both polymers. It is however worth noting that the mechanism of hydrolytic chain
527 scission was shown to be more pronounced for PBSA than PHBV (Fig. 8) due to significant
528 differences in water permeability, water diffusion and molecular weight.

529 In the first stage of degradation, PHBV mass loss increased exponentially with the
530 amorphous regions being preferentially degraded as compared to the crystalline ones. SEM
531 observations (Fig. 3) evidenced a very rough surface after primary surface erosion of PHBV
532 film, which revealed the structural organization of its crystals in spherulites. As a result, the
533 surface became porous with an important increase of the specific surface. This was expected
534 to expose more polymer chains at the film surface with as major consequence an increase of

535 the enzymatic hydrolysis rate in composting conditions, where the concentration of
536 degrading enzymes is not considered as a limiting factor. As demonstrated by DSC analysis
537 focusing on the bulk (Fig. 10-11), both amorphous and crystalline phase of PHBV seemed to
538 degrade at the same rate resulting in weak changes in crystallinity according to time, the
539 lower degradation rate of the crystalline phase being compensated by its higher area
540 revealed by the enzymatic etching of the film surface. The increase of carbonyl index during
541 this first period also emphasized the significant surface erosion of PHBV (Fig. 7). At the end
542 of this period (≈ 20 days), mass loss and CO_2 released measurements led to suppose that the
543 degradation rate reached a steady state with stabilization, and then a slow down at the end
544 of the biodegradation process (Fig. 1-2). This scenario was also in concordance with the
545 evolution of carbonyl index of PHBV, which indicated a decrease during this second phase
546 (Fig. 7).

547 By contrast, mass loss evolved almost linearly for PBSA during the first phase of degradation
548 (Fig. 1-2). The etched surface evidenced by SEM as a function of the degradation time (Fig. 3)
549 made appear crystals organized in flat layers parallel to the film surface. Such a spatial
550 organization of crystal was not prone to promote surface erosion. The crystalline phase
551 being degraded slower than the amorphous one, the surface erosion of PBSA evolved slowly.
552 The increase of carbonyl index observed during this phase was also consistent with a low
553 erosion rate of the film surface (Fig. 7). As a consequence PBSA film exhibited weak changes
554 in roughness and specific surface during this first phase. However, the propensity of PBSA to
555 become brittle instead of porous gradually led the film to fragment throughout the
556 degradation in compost (Fig. 5-6). At the end of this first phase, surface erosion and
557 fragmentation have sufficiently progressed to increase the exposition of the amorphous
558 regions of PBSA giving them more access to enzymes. This led the degradation kinetic to
559 accelerate in the second phase (>20 days) as evidenced by evolution in mass loss and
560 mineralisation rates (Fig. 1-2). As a consequence, the higher degradation rate of the
561 amorphous phase caused the crystallinity rate of the film to increase sharply. In addition, re-
562 crystallisation phenomenon induced by extra mobility of the oligomers and short polymer
563 chains generated by water-induced hydrolysis occurring in the bulk of PBSA also contributed
564 to the increase of crystallinity (Fig. 10-11). The plateau reached by the carbonyl index of
565 PBSA from 20 days emphasized the assumption that the oligomers and short polymer chains
566 produced by ester linkages hydrolysis were rapidly released from the film to be assimilated
567 in the compost medium afterwards as indicated by the mineralization curve (Fig. 2, 7).

568 Based on these two scenarios, the discrepancy in biodegradation rate between PHBV and
569 PBSA would be essentially attributed to significant differences in crystals morphology and
570 spatial organization of both polymers. Furthermore, it could not be excluded that among the
571 different microbial communities adhering on plastics, some of them possess better
572 hydrolytic capabilities regarding crystalline areas. In that regard, PHBV and PBSA films
573 displayed initially different surface properties, notably roughness and surface topography at
574 $10\mu\text{m}$ scale (Table 1). Such properties being known to control the adherence of

575 microorganisms on a surface, one can infer that the higher roughness of PBSA might hinder
576 the colonization of microorganisms at its surface [31]. This hypothesis was supported by SEM
577 images (Fig. 4) revealing footprints of microbial filaments on the surface of PHBV films
578 whereas these filaments were absent or scarcely observed on PBSA films. This led to suggest
579 that colonization of PHBV by fungi could thus have been more important than for PBSA. This
580 assumption was also supported by Mercier et al. [7], who reported that a higher microbial
581 colonization was observed for mcl-PHA than for PBS. Lastly, as shown by Song et al. [32]
582 material stiffness could also promote the colonization of the surface by microorganisms. The
583 stiffness value of PHBV being greater than these of PBSA with a young modulus of 4200 MPa
584 *versus* 290 MPa, respectively according to the furnisher specifications, this could play in
585 favour of a better propensity of PHBV to be colonized by microorganisms. The importance
586 and better degradation capability of mycelia microorganisms involved in the biodegradation
587 of plastics has already been pointed out [45] [46]. Though, mechanisms of microbial
588 adhesion in relation to polymer surface properties remain still poorly understood and would
589 need further investigations.

590 **5. Conclusions**

591 This study was performed to compare biodegradation mechanisms of two well-known
592 polymers and identify the most relevant indicators to follow biodegradation in a given
593 environment. On the strength of the results obtained and the two scenarios proposed, the
594 discrepancy in biodegradation rate between PHBV and PBSA would be essentially attributed
595 to significant differences in crystals morphology and spatial organization of both polymers.

596 Regarding the relevance of the different indicators studied, mass loss stood out as the most
597 relevant and accurate indicator to assess the disappearance of material. But, it is
598 unavoidable to associate mass loss measurements with mineralization kinetics to attest the
599 complete conversion of the polymer organic carbon into CO₂. Besides, SEM and AFM can be
600 seen as powerful tools to evidence surface erosion and morphological changes at different
601 scales. At last, changes in polymer thermal properties were shown to reflect not only surface
602 and bulk degradation, but also recrystallization phenomenon. For that regard, they appear
603 as inescapable tools for better understanding the underlying mechanisms involved in
604 polymer biodegradation. By contrast, the relevance of index carbonyl as indicator of the
605 biodegradation progress appeared less obvious since it can be interpreted differently
606 depending on the capacity of the cleaved polymer chains to be released or not from the film.
607 The same remark can be deduced from molecular weight measurements that mainly reflect
608 water-induced hydrolysis occurring in the material bulk. So, one can infer that none of these
609 two latter indicators is able to assess biodegradation or predict it.

610 **Acknowledgments**

611 The authors gratefully acknowledge Vincent Darcos (SynBio3, IBMM, Montpellier) for the
612 support provided in GPC analysis and Didier Cot (IEM, Montpellier) for SEM observations.

613 6. Bibliographic references:

- 614 [1] Geyer, R., J.R. Jambeck, and K.L. Law. Production, use, and fate of all plastics ever made. *Science*
615 *Advances*. 2017. **3**(7): e1700782.
- 616 [2] Steinbüchel, A. and T. Lütke-Eversloh. Metabolic engineering and pathway construction for
617 biotechnological production of relevant polyhydroxyalkanoates in microorganisms.
618 *Biochemical Engineering Journal*. 2003. **16**(2): 81-96.
- 619 [3] Corre, Y.-M., S. Bruzaud, J.-L. Audic, and Y. Grohens. Morphology and functional properties of
620 commercial polyhydroxyalkanoates: A comprehensive and comparative study. *Polymer*
621 *Testing*. 2012. **31**(2): 226-235.
- 622 [4] Jost, V. Packaging related properties of commercially available biopolymers – An overview of the
623 status quo. *eXPRESS Polymer Letters*. 2018. **12**(5): 429-435.
- 624 [5] Xu, J. and B.H. Guo. Poly(butylene succinate) and its copolymers: research, development and
625 industrialization. *Biotechnol J*. 2010. **5**(11): 1149-63.
- 626 [6] Hoshino, A., H. Sawada, M. Yokota, M. Tsuji, K. Fukuda, and M. Kimura. Influence of weather
627 conditions and soil properties on degradation of biodegradable plastics in soil AU - Hoshino,
628 Akira. *Soil Science and Plant Nutrition*. 2001. **47**(1): 35-43.
- 629 [7] Mercier, A., K. Gravouil, W. Aucher, S. Brosset-Vincent, L. Kadri, J. Colas, D. Bouchon, and T.
630 Ferreira. Fate of Eight Different Polymers under Uncontrolled Composting Conditions:
631 Relationships Between Deterioration, Biofilm Formation, and the Material Surface
632 Properties. *Environmental Science & Technology*. 2017. **51**(4): 1988-1997.
- 633 [8] Yang, H.-S., J.-S. Yoon, and M.-N. Kim. Dependence of biodegradability of plastics in compost on
634 the shape of specimens. *Polymer Degradation and Stability*. 2005. **87**(1): 131-135.
- 635 [9] Avella, M., E. Martuscelli, and M. Raimo. Review Properties of blends and composites based on
636 poly(3-hydroxy)butyrate (PHB) and poly(3-hydroxybutyrate-hydroxyvalerate) (PHBV)
637 copolymers. *Journal of Materials Science*. 2000. **35**(3): 523-545.
- 638 [10] Mergaert, J., C. Anderson, A. Wouters, J. Swings, and K. Kersters. Biodegradation of
639 polyhydroxyalkanoates. *FEMS Microbiology Letters*. 1992. **103**(2): 317-321.
- 640 [11] Tserki, V., P. Matzinos, E. Pavlidou, D. Vachliotis, and C. Panayiotou. Biodegradable aliphatic
641 polyesters. Part I. Properties and biodegradation of poly(butylene succinate-co-butylene
642 adipate). *Polymer Degradation and Stability*. 2006. **91**(2): 367-376.
- 643 [12] Bugnicourt, E., P. Cinelli, V. Alvarez, and A. Lazzeri. Polyhydroxyalkanoate (PHA): Review of
644 synthesis, characteristics, processing and potential applications in packaging. *eXPRESS*
645 *Polymer Letters*. 2014. **8**(11): 791-808.
- 646 [13] Tokiwa, Y., B.P. Calabia, C.U. Ugwu, and S. Aiba. Biodegradability of plastics. *International*
647 *Journal of Molecular Sciences*. 2009. **10**(9): 3722-3742.
- 648 [14] Lucas, N., C. Bienaime, C. Belloy, M. Queneudec, F. Silvestre, and J.-E. Nava-Saucedo. Polymer
649 biodegradation: Mechanisms and estimation techniques – A review. *Chemosphere*. 2008.
650 **73**(4): 429-442.
- 651 [15] Eldsäter, C., S. Karlsson, and A.-C. Albertsson. Effect of abiotic factors on the degradation of
652 poly(3-hydroxybutyrate-co-3-hydroxyvalerate) in simulated and natural composting
653 environments. *Polymer Degradation and Stability*. 1999. **64**(2): 177-183.
- 654 [16] Luo, S. and A.N. Netravali. A study of physical and mechanical properties of
655 poly(hydroxybutyrate-co-hydroxyvalerate) during composting. *Polymer Degradation and*
656 *Stability*. 2003. **80**(1): 59-66.
- 657 [17] Rutkowska, M., K. Krasowska, A. Heimowska, G. Adamus, M. Sobota, M. Musioł, H. Janeczek, W.
658 Sikorska, A. Krzan, E. Žagar, and M. Kowalczuk. Environmental Degradation of Blends of
659 Atactic Poly[(R,S)-3-hydroxybutyrate] with Natural PHBV in Baltic Sea Water and Compost
660 with Activated Sludge. *Journal of Polymers and the Environment*. 2008. **16**(3): 183-191.
- 661 [18] Weng, Y.-X., Y. Wang, X.-L. Wang, and Y.-Z. Wang. Biodegradation behavior of PHBV films in a
662 pilot-scale composting condition. *Polymer Testing*. 2010. **29**(5): 579-587.

- 663 [19] Weng, Y.-X., X.-L. Wang, and Y.-Z. Wang. Biodegradation behavior of PHAs with different
664 chemical structures under controlled composting conditions. *Polymer Testing*. 2011. **30**(4):
665 372-380.
- 666 [20] Iggui, K., N. Le Moigne, M. Kaci, S. Cambe, J.-R. Degorce-Dumas, and A. Bergeret. A
667 biodegradation study of poly(3-hydroxybutyrate-co-3-hydroxyvalerate)/organoclay
668 nanocomposites in various environmental conditions. *Polymer Degradation and Stability*.
669 2015. **119**: 77-86.
- 670 [21] Puchalski, M., G. Szparaga, T. Biela, A. Gutowska, S. Sztajnowski, and I. Krucińska. Molecular and
671 Supramolecular Changes in Polybutylene Succinate (PBS) and Polybutylene Succinate Adipate
672 (PBSA) Copolymer during Degradation in Various Environmental Conditions. 2018. **10**(3): 251.
- 673 [22] Deroine, M., G. Cesar, A. Le Duigou, P. Davies, and S. Bruzaud. Natural Degradation and
674 Biodegradation of Poly(3-Hydroxybutyrate-co-3-Hydroxyvalerate) in Liquid and Solid Marine
675 Environments. *Journal of Polymers and the Environment*. 2015. **23**(4): 493-505.
- 676 [23] Owens, D.K. and R.C. Wendt. Estimation of the surface free energy of polymers. *Journal of*
677 *Applied Polymer Science*. 1969. **13**(8): 1741-1747.
- 678 [24] Van Oss, C.J., R.J. Good, and M.K. Chaudhury. Additive and nonadditive surface tension
679 components and the interpretation of contact angles. *Langmuir*. 1988. **4**(4): 884-891.
- 680 [25] Siracusa, V., N. Lotti, A. Munari, and M. Dalla Rosa. Poly(butylene succinate) and poly(butylene
681 succinate-co-adipate) for food packaging applications: Gas barrier properties after stressed
682 treatments. *Polymer Degradation and Stability*. 2015. **119**: 35-45.
- 683 [26] Kann, Y., M. Shurgalin, and R.K. Krishnaswamy. FTIR spectroscopy for analysis of crystallinity of
684 poly(3-hydroxybutyrate-co-4 -hydroxybutyrate) polymers and its utilization in evaluation of
685 aging, orientation and composition. *Polymer Testing*. 2014. **40**: 218-224.
- 686 [27] Sedlacek, P., E. Slaninova, V. Enev, M. Koller, J. Nebesárová, I. Marova, K. Hrubanova, V.
687 Krzyzanek, O. Samek, and S. Obruca. What keeps polyhydroxyalkanoates in bacterial cells
688 amorphous? A derivation from stress exposure experiments. *Applied Microbiology and*
689 *Biotechnology*. 2019. **103**(4): 1905-1917.
- 690 [28] Nguyen, T.Q. Kinetics of mechanochemical degradation by gel permeation chromatography.
691 *Polymer Degradation and Stability*. 1994. **46**(1): 99-111.
- 692 [29] Charlon, S., N. Follain, C. Chappay, E. Dargent, J. Soulestin, M. Sclavons, and S. Marais.
693 Improvement of barrier properties of bio-based polyester nanocomposite membranes by
694 water-assisted extrusion. *Journal of Membrane Science*. 2015. **496**: 185-198.
- 695 [30] Rosa, D.S., N.T. Lotto, D.R. Lopes, and C.G.F. Guedes. The use of roughness for evaluating the
696 biodegradation of poly- β -(hydroxybutyrate) and poly- β -(hydroxybutyrate-co- β -valerate).
697 *Polymer Testing*. 2004. **23**(1): 3-8.
- 698 [31] Riedewald, F. Bacterial Adhesion to Surfaces: The Influence of Surface Roughness. *PDA Journal*
699 *of Pharmaceutical Science and Technology*. 2006. **60**(3): 164-171.
- 700 [32] Song, F., H. Koo, and D. Ren. Effects of Material Properties on Bacterial Adhesion and Biofilm
701 Formation. *J Dent Res*. 2015. **94**(8): 1027-34.
- 702 [33] Nishida, H. and Y. Tokiwa. Effects of higher-order structure of poly(3-hydroxybutyrate) on its
703 biodegradation. II. Effects of crystal structure on microbial degradation. *Journal of*
704 *environmental polymer degradation*. 1993. **1**(1): 65-80.
- 705 [34] Kijchavengkul, T., R. Auras, M. Rubino, S. Selke, M. Ngouajio, and R.T. Fernandez. Biodegradation
706 and hydrolysis rate of aliphatic aromatic polyester. *Polymer Degradation and Stability*. 2010.
707 **95**(12): 2641-2647.
- 708 [35] Deroiné, M., A. Le Duigou, Y.-M. Corre, P.-Y. Le Gac, P. Davies, G. César, and S. Bruzaud.
709 Accelerated ageing and lifetime prediction of poly(3-hydroxybutyrate-co-3-hydroxyvalerate)
710 in distilled water. *Polymer Testing*. 2014. **39**: 70-78.
- 711 [36] Wei, L. and A.G. McDonald. Accelerated weathering studies on the bioplastic, poly(3-
712 hydroxybutyrate-co-3-hydroxyvalerate). *Polymer Degradation and Stability*. 2016. **126**: 93-
713 100.

- 714 [37] Han, X. and J. Pan. Polymer chain scission, oligomer production and diffusion: A two-scale model
715 for degradation of bioresorbable polyesters. *Acta Biomaterialia*. 2011. **7**(2): 538-547.
- 716 [38] Gleadall, A. and J. Pan. Computer simulation of polymer chain scission in biodegradable
717 polymers. *Journal of biotechnology and biomaterials*. 2013. **3**(1):154-159
- 718 [39] Charlon, S., Follain, N. , Soulestin, Jérémie ; Sclavons, Michel and S. Marais. Water Transport
719 Properties of Poly(butylene succinate) and Poly[(butylene succinate)-co-(butylene adipate)]
720 Nanocomposite Films: Influence of the Water-Assisted Extrusion Process. *The Journal of*
721 *Physical Chemistry Part C: Nanomaterials and Interfaces*. 2017.**121**:918-930
- 722 [40] Crétois, R., Follain, N., Dargent, E., Soulestin, J., Bourbigot S., Marais, S., and L. Lebrun.
723 Microstructure and barrier properties of PHBV/organoclays bionanocomposites. *Journal of*
724 *Membrane Science*. 2014.**467**:56–66
- 725 [41] Messin, T., Follain, N., Guinault, A., Sollogoub, C., Gaucher, V., Delpouve, N., and S. Marais.
726 Structure and barrier properties of multilayered biodegradable PLA/PBSA films:
727 confinement effect via forced assembly coextrusion. *ACS Applied Materials and Interfaces*.
728 2017.**9**(34):29101-29112.
- 729 [42] Gan, Z., K. Kuwabara, H. Abe, T. Iwata, and Y. Doi. The role of polymorphic crystal structure and
730 morphology in enzymatic degradation of melt-crystallized poly(butylene adipate) films.
731 *Polymer Degradation and Stability*. 2005. **87**(1): 191-199.
- 732 [43] Han, X. and J. Pan. A model for simultaneous crystallisation and biodegradation of biodegradable
733 polymers. *Biomaterials*. 2009. **30**(3): 423-430.
- 734 [44] Iggui, K., M. Kaci, N.L. Moigne, and A. Bergeret. The effects of accelerated photooxidation on
735 molecular weight and thermal and mechanical properties of PHBV/Cloisite 30B
736 bionanocomposites. *Journal of Renewable Materials*. 2018. **6**(3): 288-298.
- 737 [45] Tosin, M., M. Weber, M. Siotto, C. Lott, and F. Degli Innocenti. Laboratory Test Methods to
738 Determine the Degradation of Plastics in Marine Environmental Conditions. *Frontiers in*
739 *Microbiology*. 2012. **3**: 225.
- 740 [46] Sang, B.-I., K. Hori, Y. Tanji, and H. Unno. Fungal contribution to in situ biodegradation of poly(3-
741 hydroxybutyrate-co-3-hydroxyvalerate) film in soil. *Applied Microbiology and Biotechnology*.
742 2002. **58**(2): 241-7.

743

744 LEGEND OF FIGURES

745 Figure 1: Evolution of the weight loss (%) of PBSA and PHBV films during incubation in laboratory–
746 scale compost conditions.

747 Figure 2: Mineralisation (%) of PHBV and PBSA films evaluated by monitoring CO₂ released during
748 incubation in laboratory–scale compost conditions.

749 Figure 3: SEM observations of the surface morphology of PHBV and PBSA films collected from the
750 compost medium at day 6, 10 and 20.

751 Figure 4: SEM images of PHBV and PBSA films surface evidencing footprints of microbial filaments.

752 Figure 5: Pictures of PHBV and PBSA films collected from the compost medium after 20 of incubation

753 Figure 6: SEM observation of PHBV and PBSA films collected from the compost medium at day 41.

754 Figure 7: Evolution of carbonyl index of PHBV and PBSA films during incubation in compost medium.

755 Carbonyl indexes were calculated using reference peaks at 1379 cm⁻¹ (-CH₃ symmetric wagging) for

756 PHBV and at 1473 cm⁻¹ for PBSA (-CH- symmetric deformation)

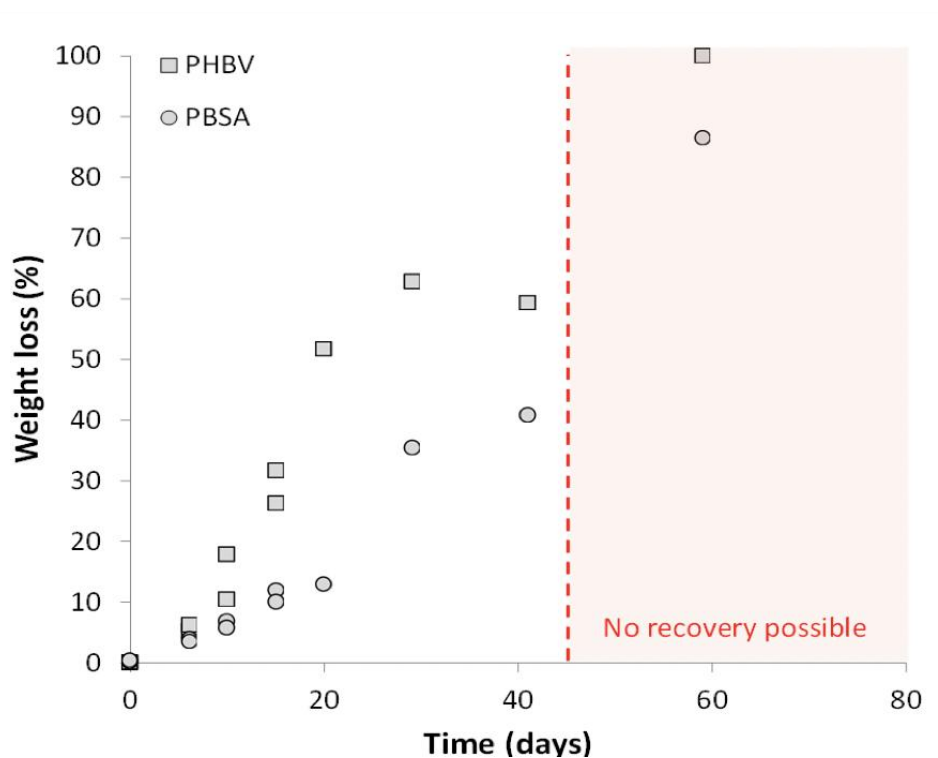
757 Figure 8: Evolution of the number-average molecular weight (M_n) of PHBV and PBSA films during
758 incubation in laboratory-scale compost conditions

759 Figure 9: Evolution of the scission index (SI) of PHBV and PBSA films during incubation in laboratory-
760 scale compost conditions

761 Figure 10: Evolution of the crystallinity rate c_c (%) of PHBV and PBSA films during incubation in
762 laboratory-scale compost conditions

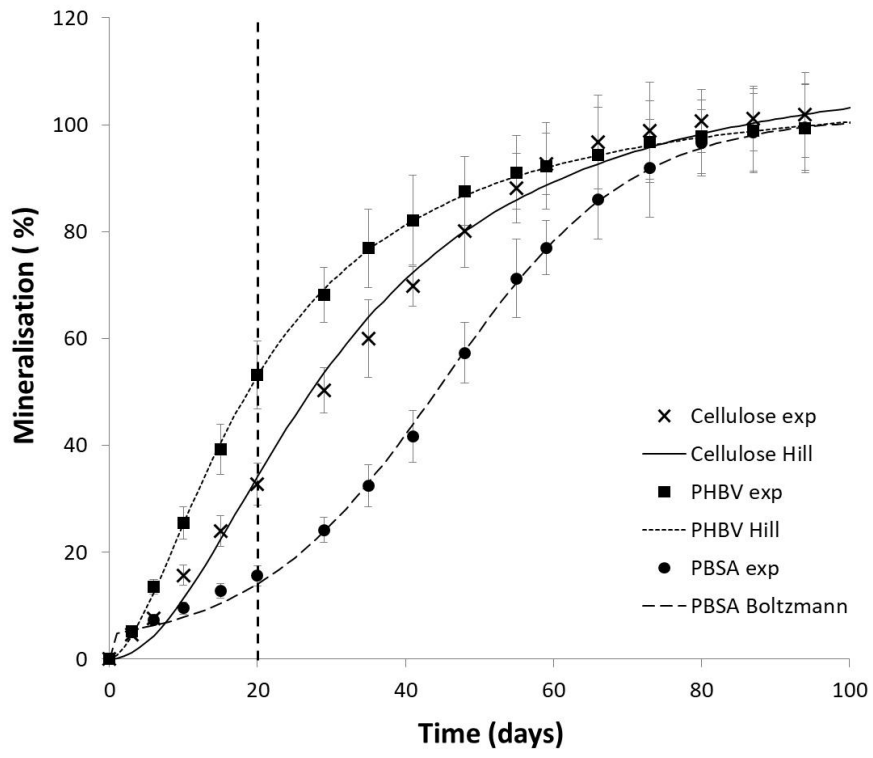
763 Figure 11: DSC melting peaks of PHBV (a) and PBSA (b) films as a function of degradation time in
764 laboratory-scale compost conditions

765 Figure 1



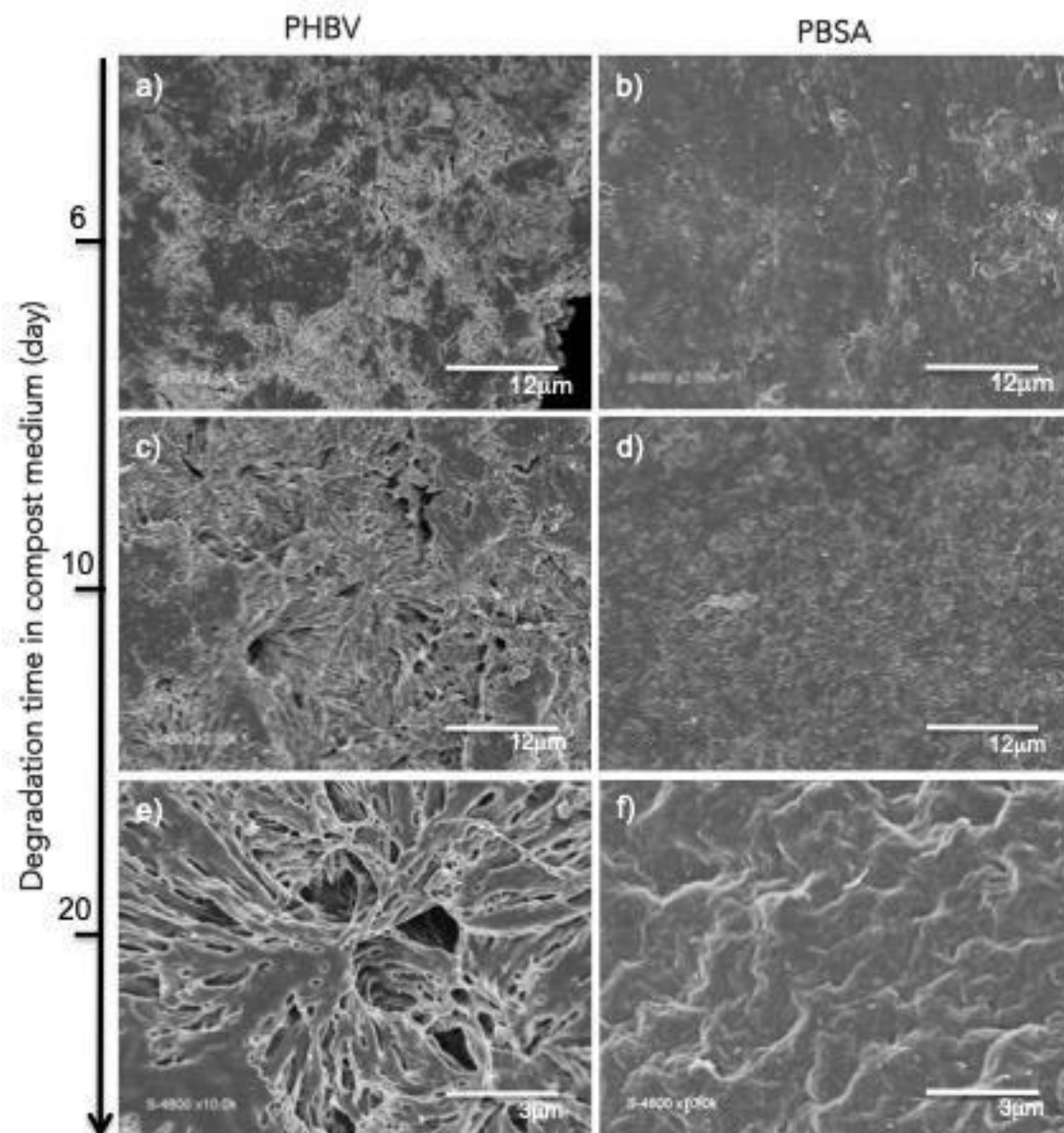
766

767 Figure 2



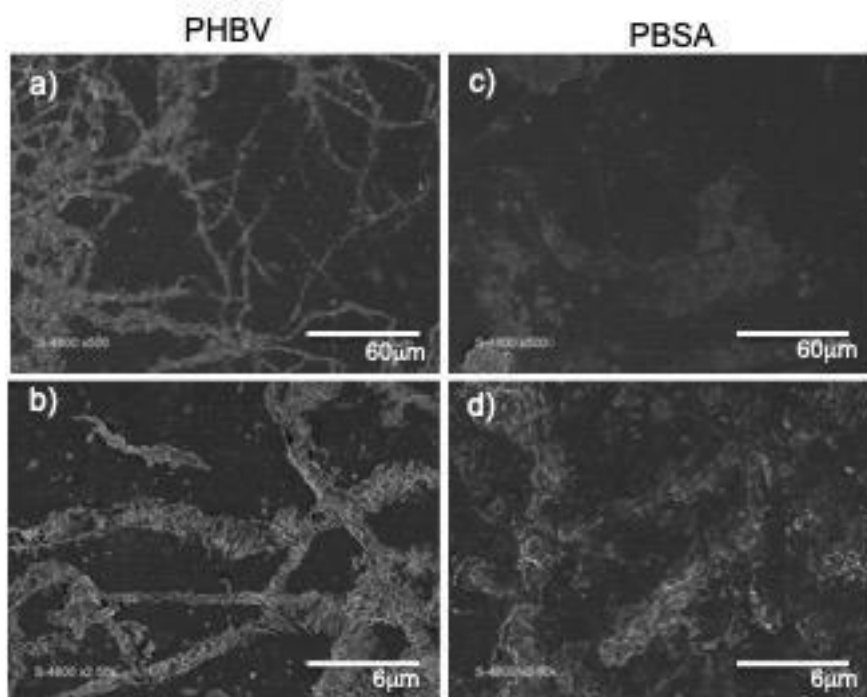
768

769 Figure 3



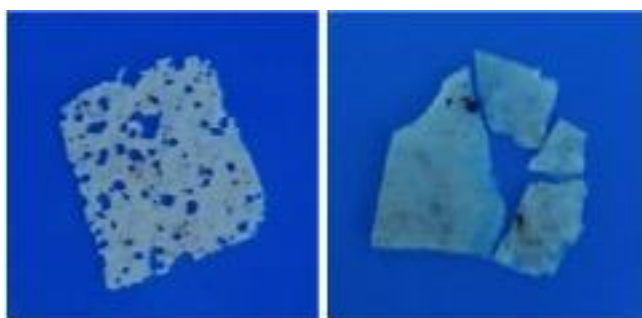
770

771 Figure 4



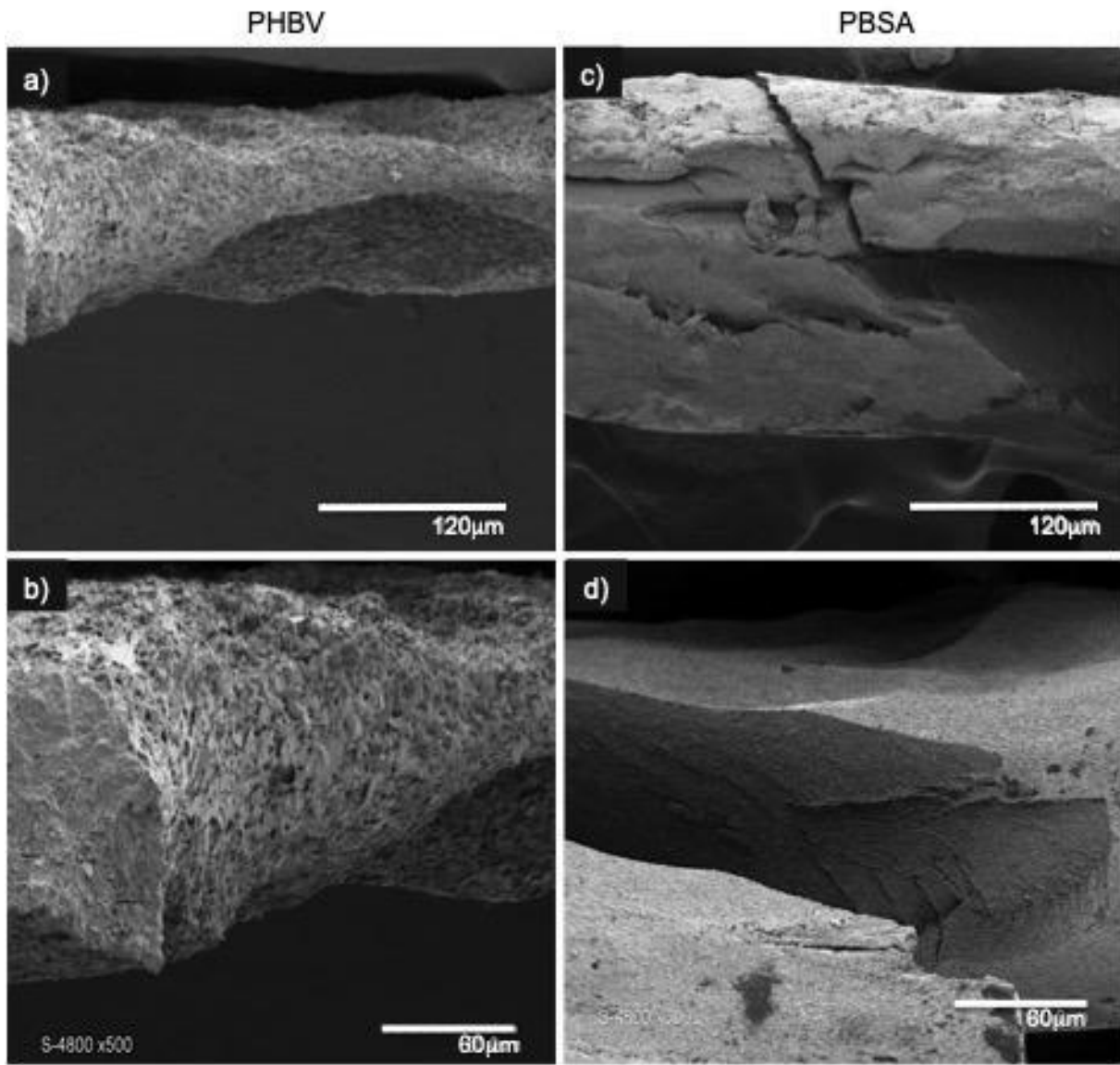
772

773 Figure 5



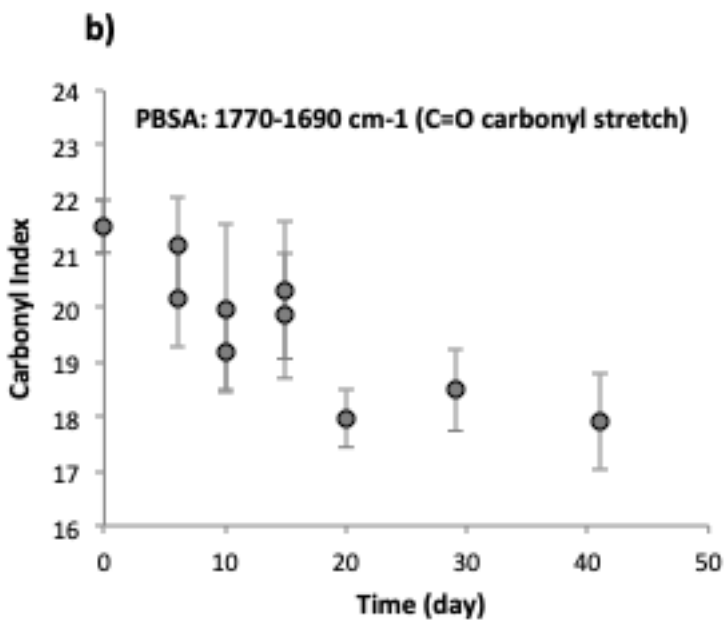
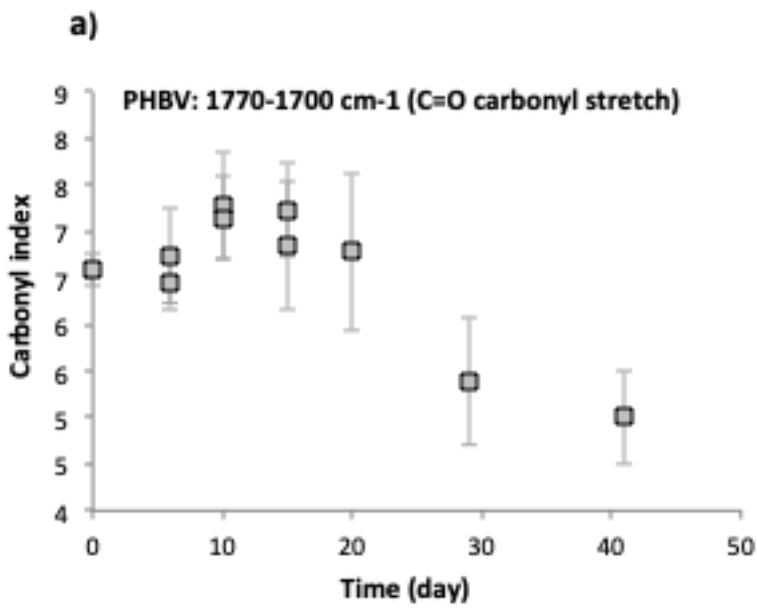
774

775 Figure 6



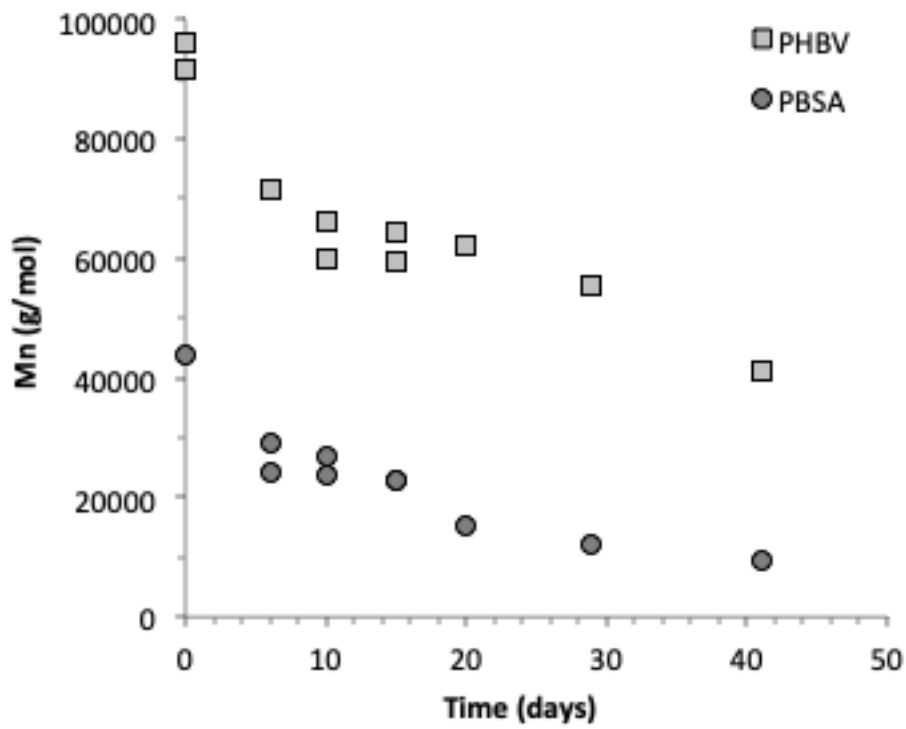
776
777

778 Figure 7



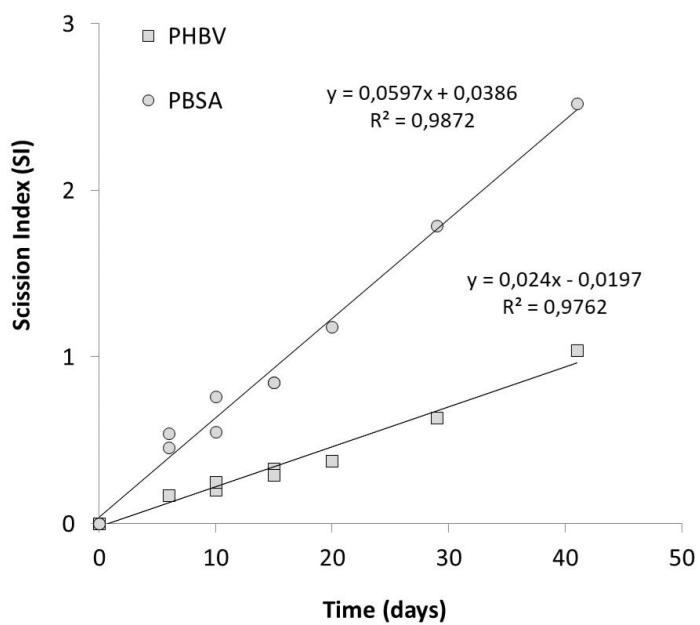
779

780 Figure 8



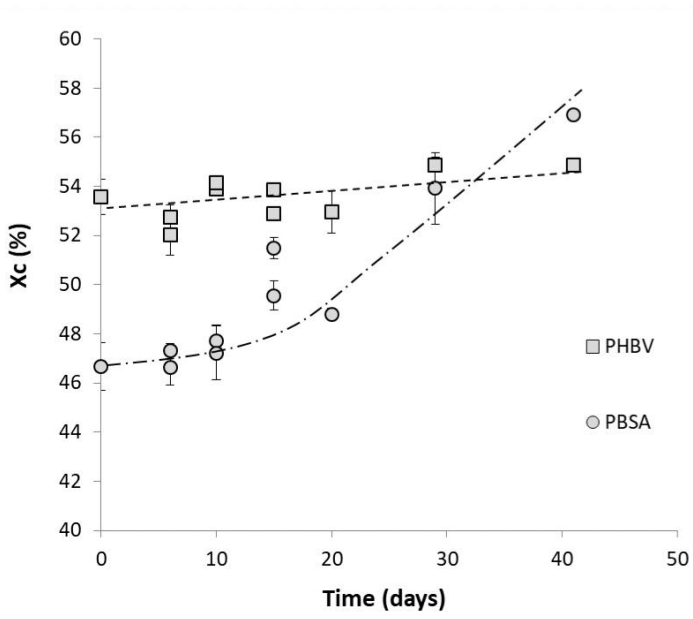
781

782 Figure 9



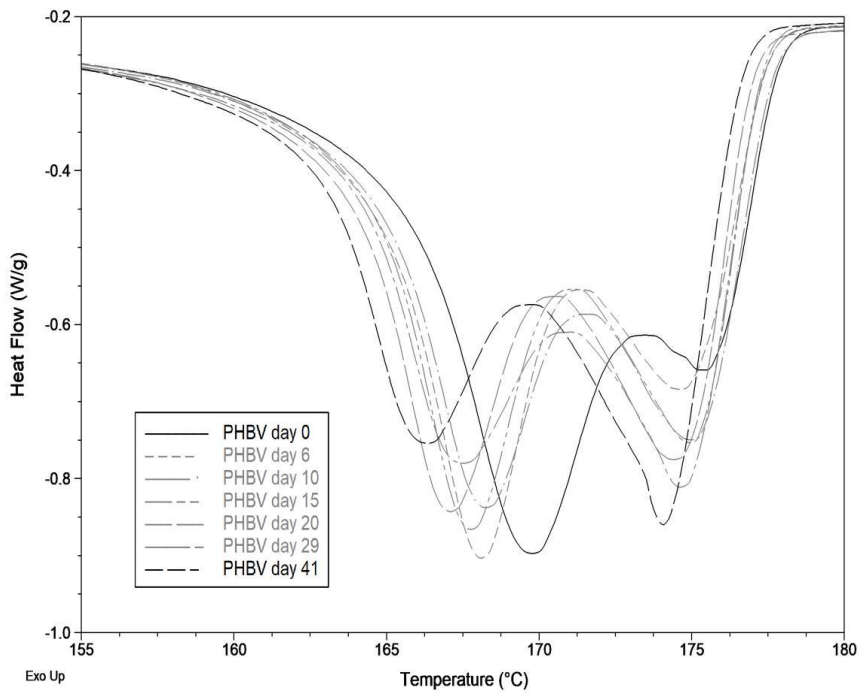
783

784 Figure 10



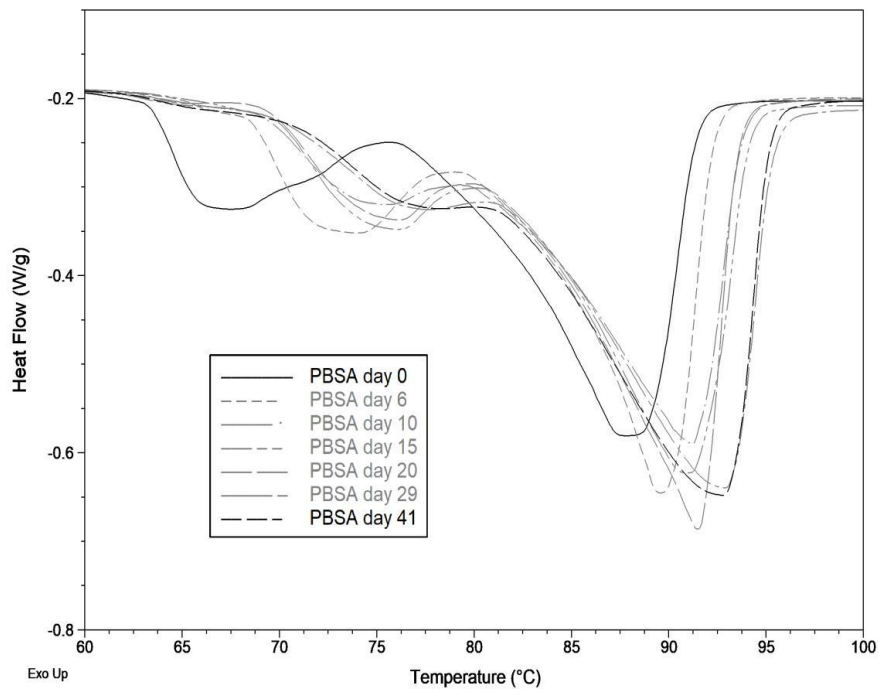
785

786 Figure 11



787

788 a) PHBV



789
790